ELSEVIER

Biochimica et Biophysica Acta 1467 (2000) 131–143

BIOCHIMICA ET BIOPHYSICA ACTA
BBA

www.elsevier.com/locate/bba

Interaction of the third helix of Antennapedia homeodomain and a phospholipid monolayer, studied by ellipsometry and PM-IRRAS at the air–water interface

E. Bellet-Amalric [a,*], D. Blaudez [b], B. Desbat [c], F. Graner [d], F. Gauthier [d], A. Renault [d,1]

[a] *Institut Laue-Langevin, 6 rue Jules Horowitz, B.P. 156, F-38042 Grenoble Cedex, France*
[b] *CNRS UMR 5798 and Université Bordeaux I, Centre de Physique Moléculaire Optique et Hertzienne, F-33405 Talence Cedex, France*
[c] *CNRS UMR 5803 and Université Bordeaux I, Laboratoire de Physico-Chimie Moléculaire, F-33405 Talence Cedex, France*
[d] *CNRS UMR 5588 and Université Grenoble I, Laboratoire de Spectrométrie Physique, BP 87, F-38402 St. Martin d'Hères Cedex, France*

Received 7 February 2000; accepted 5 April 2000

Abstract

The penetratin peptide, a 16 amino acid sequence extracted from Antennapedia homeodomain, is able to translocate across a neural cell membrane through an unknown mechanism, most likely a non-specific interaction with membrane lipids. Beyond its potential application as vector targeting small hydrophilic molecules and enabling them to reach a cell nucleus, this observation raises intriguing questions concerning the physico-chemistry of peptide–lipid interactions. Here we present a study of the role of lipid surface pressure and head charge on the mechanism of interaction. This was performed using optical techniques: surface infrared spectroscopy and ellipsometry, applied to a monolayer of phospholipids deposited at the air–water interface. Determination of the structure and orientation of peptides and lipids (separately or together) evidenced that electrostatic rather than amphiphilic interactions determine the peptide adsorption and its action on lipids.

Keywords: Penetratin; Antennapedia homeodomain; Peptide–lipid interaction; Polarisation modulation spectroscopy; Ellipsometry; Peptide structure

1. Introduction

Penetratin is the commercial name for a 16 amino acid peptide extracted from the third and fourth helices of Antennapedia homeodomain [1]. This peptide, also denoted pAntp 43–58 [2], and some of its analogs [3,4] have been shown to translocate across neural cell membranes. It can be used as a vector targeting hydrophilic molecules [5], even as large as a 20 amino acid peptide [6], to a cell cytoplasm and even sometimes to the nucleus without damaging the cell membrane, as opposed to many amphiphilic peptides which disrupt it [7,8]. These potential applications have aroused interest in this particular peptide.

The mechanism of penetration is unknown but it is

* Corresponding author. Present address: CEA, DRFMC/SP2M/SGX, 17 av. des Martyrs, F-38054 Grenoble Cedex, France. Fax: +33-476-88-50-97; E-mail: eamalric@cea.fr

[1] Present address: GMCM UMR 6626, Bat 11A, Campus de Beaulieu, F-35042 Rennes Cedex, France.

0005-2736/00/$ – see front matter
PII: S0005-2736(00)00218-2

most likely unspecific, in the sense that it is not based on any kind of shape recognition by a receptor protein: it has thus been assumed that the penetratin mainly interacts with the lipid bilayer of the membrane [4]. Such hypothesis is not unreasonable, especially considering that the penetratin is positively charged and could be attracted by negative charges in the bilayer. To understand the physical mechanism underlying these biological effects, the present paper applies a recent method to characterise the interaction between a layer of lipids and a peptide [9] to the case of penetratin.

The configuration used here, a monolayer of pure phospholipid at the air–water interface and a peptide dissolved in water, was well suited to optical techniques. Adsorption kinetics of peptides as well as formation and equilibration of monolayers in real time were recorded with ellipsometry, along with thermodynamical measurements of surface tension. In parallel, polarisation modulation infrared reflection absorption spectroscopy (PM-IRRAS) [10,11] is a new powerful technique able to detect within a few minutes the infrared absorption spectrum of a single monomolecular layer; it is sensitive to the composition, amount, orientation and conformation of adsorbed peptides or lipids alone, and also of mixed peptides and lipids.

This paper concerns the interaction between the peptide and lipidic monolayers. A complementary study, using neutron reflectometry, investigated the interaction with a single controlled bilayer deposited on a solid substrate [12]. The test of its ability to cross such a model membrane, or the comparison with control peptides lacking its properties, are out of the scope of this paper (work in progress).

2. Materials and methods

2.1. Chemicals

Abbreviations: penetratin, Arg-Gln-Ile-Lys-Ile-Trp-Phe-Gln-Asn-Arg-Arg-Met-Lys-Trp-Lys-Lys, $M = 2246.7$ g/mol. Lipids: DPPC, di-palmitoyl phosphatidyl-choline; DPPS, di-palmitoyl phosphatidyl-serine. Subphase: PBS (phosphate-buffered saline), solution of 9 g/l NaCl, 13.61 g/l KH_2PO_4, 3.2 g/l NaOH, pH 7.3.

Water and peptide solutions were freshly prepared with pure water (18 MΩ cm, Elga or Milli-Q, Millipore). PBS was chosen as the buffer subphase since phosphate ions are visible in infrared spectra but do not hinder the measurements. The penetratin peptide was synthesised by Neosystem; the purity as checked by high performance liquid chromatography and mass spectroscopy was 95%. Initially the counter-anion was tetra-fluoro-acetate, which is not suitable for infrared spectroscopic studies. According to Neosystem's indication, we thus resuspended the peptide in excess HCl, 0.1 M (the peptide was not modified and all counter-anions were exchanged by Cl^-, as checked by mass spectroscopy and infrared spectroscopy), and lyophilised it.

Experiments with lipids (Avanti Polar Lipids) were conducted with the zwitterionic phosphatidyl-choline heads since it is a dominant component of membranes, and phosphatidyl-serine in order to test the effect of negative head charges. An identical tail length of 16 carbons allowed a comparison between different polar heads. Saturated tails have the advantage of being stable in time; lipids with 16 carbon chains are insoluble and thus form stable monolayers. For spectroscopy, perdeuterated (d-75) DPPC and chain deuterated (d-62) DPPS were used. DPPC was purchased as powder and dissolved in chloroform according to the indications of the manufacturer. DPPS was purchased dissolved in chloroform–methanol and used without further purification.

2.2. Spectroscopy measurements

The principle and experimental set-up of PM-IRRAS have been described in detail elsewhere [10,11]. Briefly, PM-IRRAS combines Fourier transform infrared (FT-IR) reflection spectroscopy with fast modulation of the polarisation of the incident beam between parallel (p) and perpendicular (s) directions. The two-channel processing of the detected signal gives the differential reflectivity spectrum $\Delta R/R = (R_p - R_s)/(R_p + R_s)$. To remove the contribution of water absorption, the spectra are divided by those of the subphase: they are expressed in PM-IRRAS units, which are dimensionless but not arbitrary. With an angle of incidence of 75°, transition moments in the interface plane give strong and upwards

oriented bands, while transition moments perpendicular to the interface give weaker and downwards oriented bands.

Spectroscopic measurements were performed on a 29×10 cm^2, 160 ml rectangular Teflon Langmuir trough with a computer controlled barrier (Nima). Surface tension γ was measured with a plate of filter paper held by a Wilhelmy balance. Spectra were recorded, with an 8 cm^{-1} resolution on a Nicolet 740 spectrometer equipped with a liquid nitrogen cooled HgCdTe detector. For equilibrium spectrum, 400 scans were recorded in 10 min; out of equilibrium spectrum were obtained by adding 80 scans (acquisition time 2 min, repetition time 3.5 min). The infrared beam probed a surface of about 1 cm^2. The spectrum and γ_0 of the pure subphase were taken and used as a reference, to divide further spectra and to record the surface pressure $\Pi=\gamma_0-\gamma$, respectively.

Deuterated lipids were used to distinguish them from the peptide. The deuteration of the lipids had a second advantage: since the frequencies of CD_2 bands are closer to the interesting region of amide bands than the CH_2 bands are, CD_2 and amide bands could be simultaneously recorded in the same spectrum by optimising the spectrometer over the 900–2300 cm^{-1} region. We checked that the thermodynamical behaviour of the peptide, and the spectra of the other bands, were unaffected by this deuteration.

For experiments on peptide alone, a solution of peptide in pure water (1–3 mg/ml) was prepared and injected at a concentration c (μmol/l PBS) until equilibration. When compression isotherms were performed with the barrier, out-of-equilibrium spectra were recorded.

For peptide–lipid mixtures, lipids were spread first until Π became measurable (>0.1 mN/m) and equilibrated for half an hour until the solvent evaporated. An isotherm was recorded while lipids were compressed to the desired initial pressure Π_{lip} and a spectrum of pure lipids was taken as reference. The peptide was then injected in the water by successive additions up to a bulk concentration c. When in 'constant Π' mode, the pressure was regulated at fixed value $\Pi=\Pi_{lip}$ by the movable barrier. After each addition of peptide, the trough area A and spectra were recorded during equilibration until the variations of A during the spectrum acquisition were only a fraction of a percent and until two successive spectra were indistinguishable. At each peptide injection, the syringe removed from the monolayer a small amount of lipids: this effect was estimated by injecting pure water as a control, and was taken into account in subsequent measurements of A.

For the bulk pure peptide, absorbance spectra were obtained by conventional transmission spectroscopy.

2.3. Quantitative analysis

Band positions, widths and integrated intensities I were determined after baseline subtraction using a spectral decomposition software (Grams from Galactic, USA). The amide III spectral region (1320–1220 cm^{-1}) could only be analysed qualitatively, while the amide I–amide II spectral region (1700–1480 cm^{-1}) was intense enough for quantitative decomposition. The separation into individual bands was performed and analysed as a sum of Gaussian/Lorentzian curves. The number of bands was fixed to nine (see Table 1 for assignment):

- Five bands within the amide I region, 1628–1691 cm^{-1}, which are analysed in Section 2.4.
- Two subbands in the amide II region, 1510–1560 cm^{-1}, which were not assigned separately, and thus were not later corrected to account for orientation.
- Two lysin bands around 1501 and 1590 cm^{-1}, too weak for quantitative analysis.

The absolute and relative errors on I were, respectively, estimated to be ±0.5 U and $\pm5\%$, mainly due to the baseline subtraction. Each band intensity combined the information on molecular orientation and on the amount of molecules adsorbed within the infrared laser spot. These contributions could be separated in two ways. When a chemical group gives two bands with well known direction of the transition moment, the orientation can be determined by the ratio of both band intensities and its comparison in different conditions, for example between the bulk and the monolayer. Alternatively, in the 'constant Π' mode, the number of lipid molecules remains constant and their density varies with the area; we thus

calculated the normalised intensities $I' = I(A/A_0)$, where A_0 is the area before peptide injection.

2.4. Determination of secondary structure proportions

The integrated intensity of PM-IRRAS bands within the amide I region cannot directly give the proportion of each secondary structure. Indeed, the PM-IRRAS intensity I_i of a given secondary structure i can be written as: $I_i \propto f_i(\theta) n_i M_i$ where $f_i(\theta)$ is the orientation function of the transition moment of the amide I vibration corresponding to the structure i; n_i is the number of probed amide groups having the structure i and M_i is the magnitude of the transition moment of the amide I in the structure i. Most of the time it is assumed that transition moments corresponding to the different structures have the same magnitude. This has been recently experimentally checked, at least for α-helix and β-sheet secondary structures [13]. Thus, we will not take the parameter M_i into account. The determination of n_i can be achieved only if the orientation function is known. We will see in Section 3.2 that the case of penetratin is simple enough to draw a good estimation of these functions from spectroscopic data. The number of amide groups having the structure i is thus written: $n_i \propto (I_i/f_i(\theta))$ and the proportion of the secondary structure i is:

$$P_i(\%) = \frac{n_i}{\sum_k n_k} = \left(\frac{I_i}{f_i(\theta)}\right) \Big/ \left(\sum \frac{I_k}{f_k(\theta)}\right) \quad (1)$$

where $\Sigma_k n_k$ is the total number of amide groups probed by the IR beam.

2.5. Ellipsometry

A home-made ellipsometer [14] used a He–Ne laser ($\lambda = 632.8$ nm, Spectra-Physics) polarised with the aid of a Glan-Thompson polariser. The incidence angle of the light on the surface was 1° away from the Brewster angle. After reflection on the water surface, the laser light passed through a $\lambda/4$ retardation plate, a Glan-Thompson analyser and a photomultiplier. Through a computer controlled feedback loop, the analyser automatically rotated towards the extinction position. In this 'null ellipsometer' configuration [15], the analyser angle, multiplied by two, yielded the value of the ellipsometric angle Δ, i.e. the phase difference between parallel and perpendic-

Table 1
Positions and assignments of the individual PM-IRRAS bands mentioned in this paper

Molecule	Band	cm^{-1}	Origin	Axes	Comment
Peptide	amide I	1690	anti//β-sheet	*x*	weak
	amide I	1679	β-turn	*y*	weak
	amide I	1650[a]	α-helix	*xyz*	strong
		1650[a]	anti//β-sheet	*z*	neglected
		1644[a]	random	*xyz*	strong
	amide I	1631–34	//β-sheet	*y*	not seen
	amide I	1628	β-sheet	*y*	strong
	$\delta_a NH_3^+$	1590	lysin		weak
	amide II	1540[b]	δNH–δCN	*xz*	strong
	amide II	1520[b]	δNH–δCN	*yz*	weak
	$\delta_a NH_3^+$	1501	lysin		weak
	amide III	1300	α-helix	*xyz*	not seen
	amide III	1224	β-sheet		strong
Deuterated lipids	$\nu_a(CD_2)$	2195	chain		strong
	$\nu_s(CD_2)$	2090	chain		strong
	$\nu(C=O)$	1738	ester		strong
	$\nu_a(PO_2)$	1220–1234	head		strong
Buffer	$\nu_a(HPO_4^=)$	1080			± 20 cm^{-1} due to TO–LO splitting

See Section 2 for details and Fig. 9 for orientation of axes.
[a] Bands not resolved separately.
[b] Bands resolved but not assigned separately.

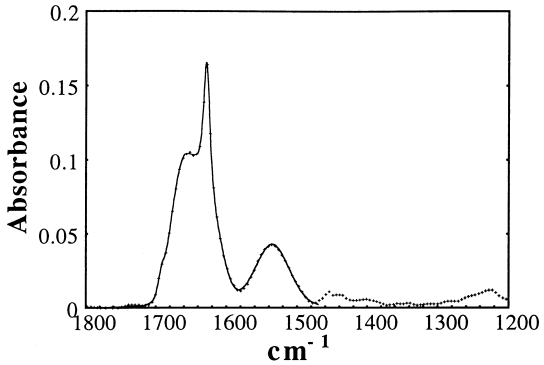

Fig. 1. IR absorption spectrum of pure peptide in bulk state (crosses). The best decomposition of the amide I and II domain 1480–1700 cm^{-1} (solid line) corresponds to the frequencies and intensities listed in Table 2.

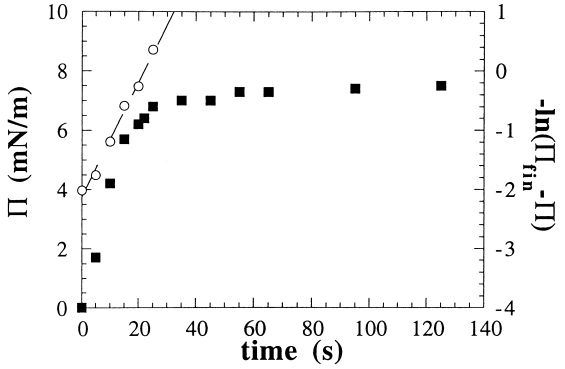

Fig. 2. Adsorption kinetic of peptide injected at $t=0$ in PBS at bulk concentration $c=1.88$ μM. Solid squares: Π; open circles: $-\ln(\Pi_{fin}-\Pi)$ and its linear fit over the first points (dashed line), the slope is 0.1 s^{-1}.

ular polarisations of the reflected light. The laser beam probed a surface of 1 mm^2 and a depth in the order of 1 μm. The surface tension was measured with a platinum plate held by a balance (Sartorius). Initial values Δ_0 and γ_0 of the ellipsometric angle and surface tension were recorded on the subphase for half an hour. These values, including a small correction for the drift due to water evaporation, have been subtracted from all data presented below. Values of Δ and Π were stable and recorded every 100 s with a precision of $\pm 0.2°$ (1/20th of a dense monolayer) and ± 0.1 mN/m, respectively.

3. Results

3.1. Pure peptide in bulk state

The spectrum of the pure powder peptide was recorded in the bulk state (Fig. 1 and Table 2) and used for further comparison. In the powder state, there is no need to correct for orientation because the orientation distribution of crystallites is isotropic. The integrated intensity decomposition indicates that 44% of amide groups are in a β-sheet structure. They are mostly antiparallel as indicated by the ratio $I_{1628}/I_{1690} \approx 10$ which is very close to the value obtained for pure antiparallel β-sheet [16]. On the other hand 33% of the groups are in β-turns and the remaining bonds are half α-helices, half random coils (11% each).

3.2. Pure peptide monolayers at the air–water interface

Successive injections of peptide at constant area resulted first in an adsorption to the air–water interface, detected by an increase in both Δ and Π. The time-scale of such absorption is in the order of 10–15 s (Fig. 2). The equilibrium surface pressure increased abruptly at $c=0.15\pm0.1$ μM, reached 2 mN/m at $c=0.3\pm0.1$ μM and continued increasing without visible saturation (Fig. 3). Nevertheless, at $c=1.5$ μM the peptide formed a complete monolayer as

Table 2
Positions and intensities of individual FT-IR Amide I bands for the peptide in the bulk state

Origin	β-Sheet anti//	β-Turn	α-Helix	random coils	β-Sheet
Frequency (cm^{-1})	1690.7	1666.2	1651	1642	1628.6
Integrated absorbance (a.u.)	0.303	2.49	0.822	0.858	3.33
%		33	11	11	44

The proportions of the four types are deduced from the intensities. Note that the β-turn band is at 1666 cm^{-1} while the PM-IRRAS band in monolayers is at 1679 cm^{-1} (see Table 1). The frequency differences for the other bands do not have any physical significance.

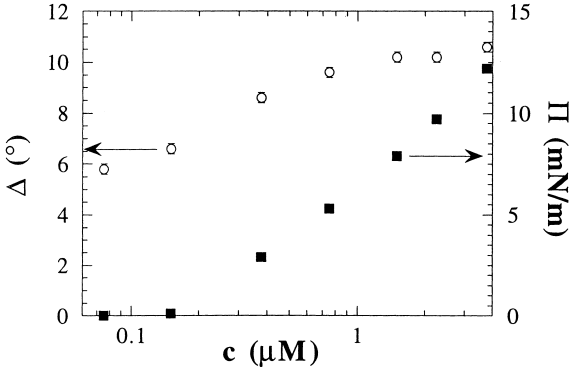

Fig. 3. Formation of a peptide monolayer by successive injections. Ellipsometric angle Δ (open circles) and surface pressure Π (solid squares) at equilibrium for different values of the bulk peptide concentration in pure PBS. Note the semi-log scale. The values of Δ and Π at $c=0$ were substracted.

evidenced by a saturation in Δ at around 11° (Fig. 3). This monolayer can be compressed up to 50 mN/m without displaying any saturation in Π (Fig. 4) (above 50 mN/m the method for measuring the pressure becomes questionable [17]). The monolayer was visibly rigid. It was not at equilibrium: Π decreased as soon as the barrier stopped compressing and displayed a strong hysteresis during decompression, the difference between $\Pi_{initial}$ and Π_{final} through a cycle being $\sim$4 mN/m. The maximum equilibrium pressure we could reach after compression and relaxation was 26 mN/m.

The equilibrium PM-IRRAS spectrum of a pure peptide film, at the air–water interface, at $\Pi=5$ mN/m (Fig. 5) clearly showed a predominance of antiparallel β-sheets and β-turns. The amide III band was clearly visible although weak (0.01 units)

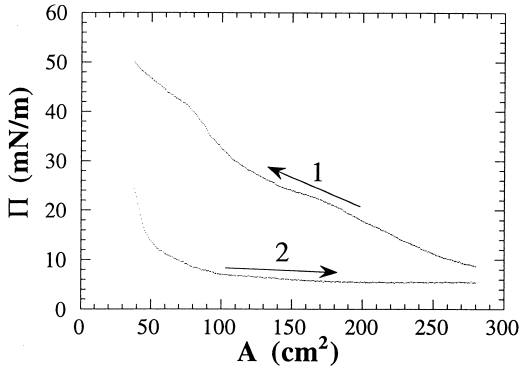

Fig. 4. Π–A isotherm of peptidic film formed at the air–water interface. $c=1.88$ μM. (1) Compression at 11 cm^2/min. (2) After 25 min relaxation, decompression at 11 cm^2/min.

at the β-sheet frequency of 1224 cm^{-1}, and was not visible at 1300 cm^{-1}. The predominance of β-sheets had also a quantitative signature: the 1628 cm^{-1} band peaks at 0.4 units. This value was comparable to the peak value at 0.37 units that Castano et al. [9] have observed on artificial 100% β-sheets. This observation indicates that the β-sheets most likely lay flat at the water surface.

To determine the secondary structure proportions we need the orientation functions of each structure (see Section 2.4). The flat orientation of the β-sheets leads to a value of one for both the β-sheet (1628 cm^{-1}) and β-turn (1679 cm^{-1}) bands. Concerning α-helix, its transition moment is composed of three non-equivalent components along the molecular axes [13]. Assuming that the helices are also oriented flat on the surface the corresponding orientation function is equal to about 4/3. On the other hand, the transition moment of a random coil is isotropic and the associated orientation function is equal to 2. Since the bands attributed to α-helices (1650 cm^{-1}) and coils (1644 cm^{-1}) are in the minority and cannot be resolved, they are lumped into a single band $I_{1644-50}$ referred below as to 'other than β-structures' with a mean orientation function equal to 5/3, assuming that the portions of helices and coils are equal (this assumption does not affect much the results). We thus calculated the orientation corrected amide I intensity as:

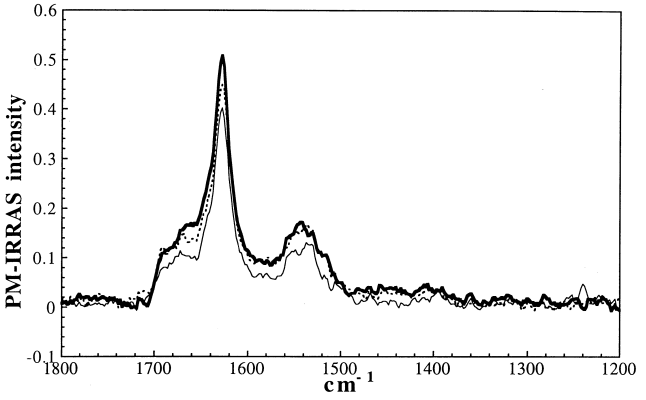

Fig. 5. PM-IRRAS spectra of pure peptide films in situ at the air–water interface. Peptide was injected in the subphase and equilibrated during 45 min ($\Pi=5$ mN/m at equilibrium, thin solid line), then compressed at 5 cm^2/min (dots: $\Pi=13.2$ mN/m; thick line: $\Pi=33.2$ mN/m). Subphase: PBS, pH = 7.2, $T=25$°C; $c=0.7$ μM.

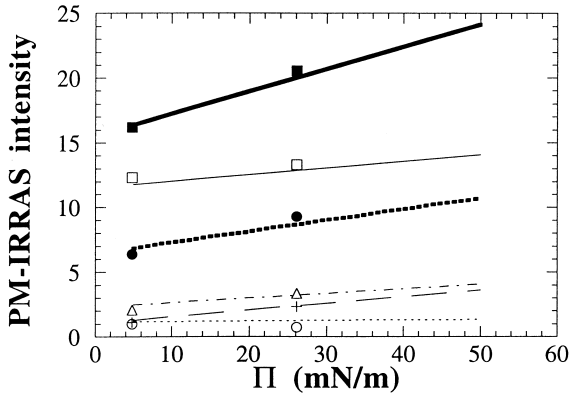

Fig. 6. Structure of the peptide at the air–water interface. The lines correspond to a linear interpolation of the out-of-equilibrium intensities of amide I and amide II bands (and subbands) of the peptide at the air–water interface, recorded during three different compressions at 5, 5 and 11 cm^2/min respectively. The agreement with measurements at equilibrium (symbols) is good. Legend: thick solid line, closed squares: $I_{1,or}$; thick dots, closed circles: I_2; thin solid line, open squares: I_{1628}; long dashes, crosses: $I_{1644-50}$; dash-dots, open triangles: $I_{1670-80}$; dots, open circles: $I_{1690-93}$.

$$I_{1,or} = \sum_k \frac{I_k}{f_k(\theta)} = I_{1628} + \frac{5}{3} I_{1644-50} + I_{1679} \qquad (2)$$

and the proportion of each secondary structure following Eq. 1.

While compressing the monolayer, the spectrum of the pure peptide film was barely affected, despite drastic changes in the surface pressure (Fig. 5). Moreover, whether at low or high barrier speed, the quantitative analysis of out-of-equilibrium spectra revealed, during compression, a linear increase of the amide I and II bands and its subbands (with a dispersion comparable to the individual error bar). In Fig. 6 we present the interpolated straight lines together with the equilibrium measurements which also fell on the same lines.

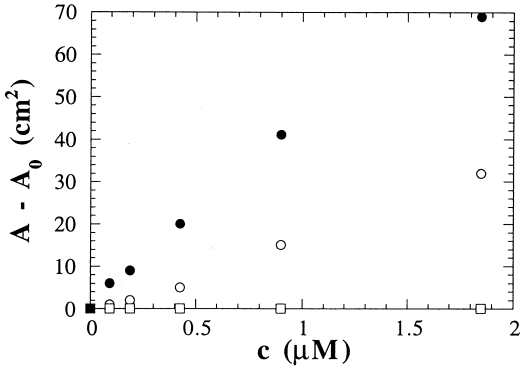

Fig. 7. Adsorption of peptide in presence of lipids. Increase in area $A–A_0$ at constant surface pressure versus bulk peptide concentration c, for DPPC (open circles at $\Pi_{lip} = 13$ mN/m, open squares at $\Pi_{lip} = 27$ mN/m) and 90% DPPC+10% DPPS (closed circles at $\Pi_{lip} = 13$ mN/m).

The analysis of these interpolations (see Table 2) reveals an important increase, from 5 to 50 mN/m, of the amide I and II intensities $I_{1,or}$, I_2, of 47% and 57% respectively (Fig. 6). This increase was correlated with the peptide density (hence with the decrease of molecular area S_{mol} calculated from ellipsometry); as expected for a soluble molecule, it was independent from the trough area A.

The decomposition of the amide I band indicated that the fraction of β-sheets and turns were respectively 72% and 15% at low pressure, i.e. a β-sheet/β-turn ratio of 4.7 and 58% and 17% at high pressure with a β-sheet/β-turn ratio of 3.5 (Table 3 and Fig. 6). If a peptide molecule made an intra-molecular β-sheet in a 'hairpin-like' shape, two or three amide groups would be in a β-turn configuration. Thus for a 16 amino acid peptide molecule, we could expect the ratio β-sheet/β-turn to lie within the interval [13/3;14/2] = [4.3;7]. When the molecule is tilted both bands are affected, but we lack the necessary information to perform the correction. We assume that their ratio is only slightly modified.

Table 3
Amide I and amide II band intensities, percentage of β-sheets, β-turns and ratios for the peptide at the air–water surface

Π (mN/m)	$I_{1,or}$ (pm-irras u.)	I_2 (pm-irras u.)	β-Sheets (%)	β-Turns (%)	β-Sheets/β-turns
5	16.4	6.8	72	15.2	4.7
50	24.1	10.7	58.3	16.9	3.5

These data come from the interpolation shown in Fig. 6.

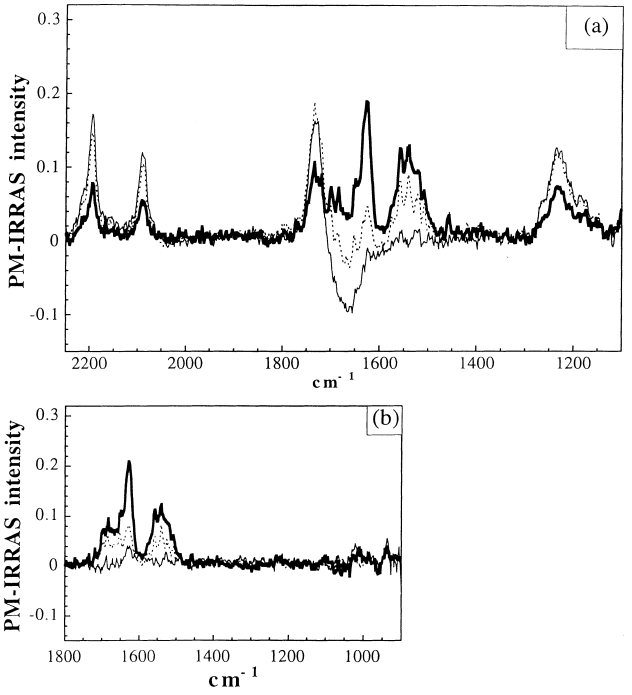

Fig. 8. Spectroscopic data of mixed peptide and DPPC lipids. (a) Equilibrium spectra of a lipidic film at 13 mN/m with peptide injected at bulk concentration $c = 0.1$ (thin solid line), 0.43 (dots) and 1.85 μM (thick line). (b) Same spectra after subtraction of the area normalised pure DPPC spectrum. (c) Analysis of the spectra vs. peptide concentration: (Top) Amide I $I'_{1,or}$ (squares) and amide II I'_2 (circles) intensities; at $c \leq 0.2$ μM, the peptide bands were visible but too weak for quantitative analysis. (Middle) Percentage of β-sheets (squares) and β-turns (triangles); arrows mark the proportions of β-sheets (s) and β-turns (t) in the bulk, see Table 2. (Bottom) Effect on the lipid intensities I' of $\nu(C=O)$ (squares), ν_a (triangles) and $\nu_s(CD_2)$ (circles).

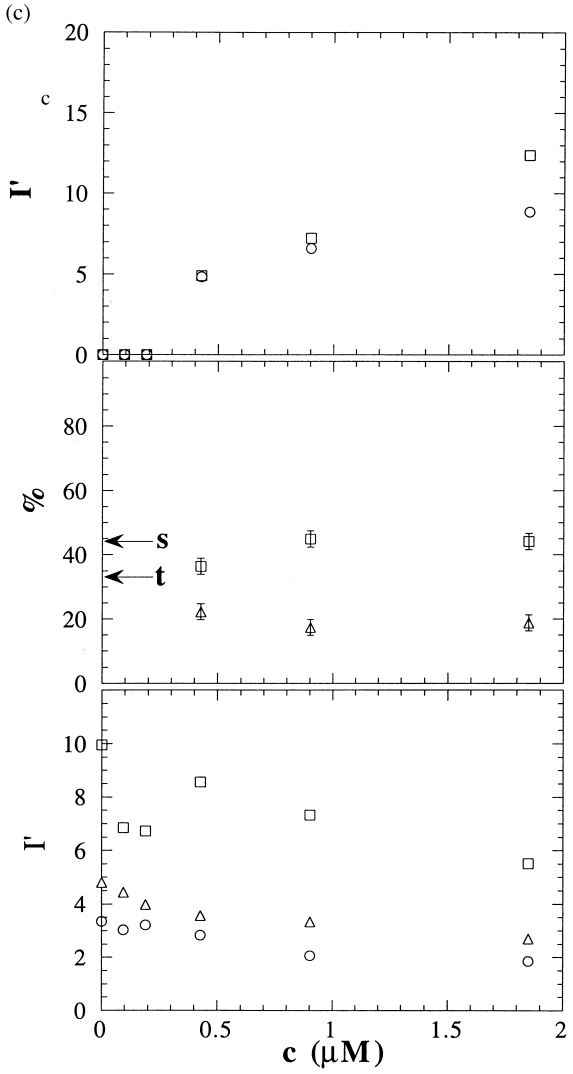

Fig. 8 (*continued*).

3.3. Peptide–lipid monolayers at the air–water interface

3.3.1. Peptide and DPPC at constant area

In the 'constant A' mode, a pure DPPC monolayer was deposited, then compressed up to the desired surface pressure Π_{lip} ($\Pi_{lip} = 0$ would denote the pure peptide case). Successive injection of peptide was done in the subphase while A was kept constant. The pressure increased with the peptide concentration c. This peptide adsorption was maximal for a DPPC pressure $\Pi_{lip} \sim 10$–15 mN/m, reaching $\Pi \sim \Pi_{lip} + 10$ mN/m and $\Delta \sim \Delta_{lip} + 10°$. Increasing the lipid pressure, the DPPC monolayer became almost insensitive to peptide (and no peptide showed at the surface) at a pressure $\Pi_{lip} \sim 27$–30 mN/m (data not shown).

3.3.2. Peptide and DPPC at constant pressure

In the 'constant' Π mode a DPPC monolayer was deposited and compressed at the desired Π_{lip}. Successive injection of peptide was done in the subphase while Π was kept constant. As expected, at high pressure $\Pi_{lip} = 27$ mN/m, the area A did not vary although it was allowed to do so: there was no peptide absorption and the lipid spectra were not affected (Fig. 7).

At $\Pi_{lip} = 13$ mN/m, when the peptide was injected in the water, the film area A varied linearly with the bulk peptide concentration c (Fig. 7). The adsorbed

peptide had a clear signature in the PM-IRRAS spectra, in the amide I and II region (Fig. 8a). Indeed, at the lowest concentration $c = 0.1$ μM, the peptide was already visible (Fig. 8b) as seen in the difference with respect to the pure lipids reference. At higher concentrations, the peptide contribution was large enough to be quantitatively decomposed: both amide I and II band intensities increased significantly with c (Fig. 8b). Since, in addition, the area increased too (Fig. 7) it revealed a large increase in the (physically relevant) normalised intensities $I'_{1,or}$ and I'_2 (see Fig. 8c). The decomposition into subbands indicated a roughly constant 42% of antiparallel β-sheets, 19% of β-turns (Fig. 8c), and 39% proportion of other structures.

When a peptide molecule is in a β-sheet structure we define its plane xy with x along the peptidic chain and y along the hydrogen bonds (see Fig. 9). When the molecule is flat xy corresponds to the XY plane of the water. According to the PM-IRRAS selection rule [10,11], if the molecules tilt around the Y axis (tilt angle (xX)) I'_{1690} decreases whereas I'_{1628} remains unchanged. On the contrary, if molecules tilt around the X axis (lateral inclination (yY)) I'_{1628} decreases whereas I'_{1690} remains constant. Comparing to the peptide alone the I'_{1628} was about six times smaller while the I'_{1690} did not significantly change. It is probably due to a lateral inclination of the molecule.

We can also analyse the effect of the peptides on the lipids using the deuterated DPPC bands (cf. Table 1). Since we observed no change in frequencies, they were direct markers of lipid orientation. For the $\nu_a(PO_2)$ band, I' displayed no significant variation (not shown). On the other side, for the ester $\nu(C=O)$, and the chains ν_a and $\nu_s(CD_2)$ bands, I' underwent a marked decrease of about $\sim 45\%$ with the peptide concentration (see Fig. 8c).

3.3.3. Peptide and 90% DPPC+10% DPPS

Mixing 10% negatively charged DPPS to the DPPC monolayer resulted in marked changes. As expected from its positive charge, more peptide adsorbed. This was visible not only in the area changes (Fig. 7) but also directly in the peptide amide I and II bands (Fig. 10a).

Moreover, on the spectra, the $\nu_a(HPO_4^=)$ band at 1080–1085 cm^{-1} appeared, indicating an adsorption

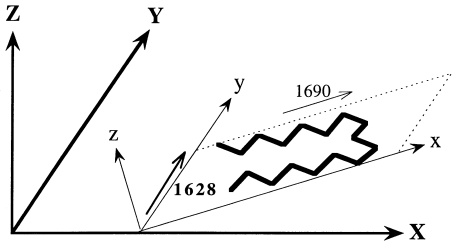

Fig. 9. Orientation of β-sheets: explanation of the notations used in the text. XYZ are fixed directions: the XY plane is the surface of water, Z the vertical. xyz is linked with the peptide molecule: x is along the peptidic chains (bold lines), so that xX is the tilt angle; y is along the hydrogen bonds, so that yY is the lateral inclination; z perpendicular to the plane of the β-sheet. The main antiparallel β-sheet amide I band at 1628 cm^{-1} is along y, the weak components at 1690 cm^{-1} is along x.

of phosphate counter-ions. When peptide was added, this band grew: phosphates probably rose to screen the highly charged peptide layer. Its growth was so intense that eventually it split in two bands (see Fig. 10b): a positive band at 1063 cm^{-1}, and a negative band at 1100 cm^{-1} in perfect agreement with simulations of PM-IRRAS spectra of the $\nu_a(HPO_4^=)$ band presenting a TO–LO splitting [18]. The explanation of this splitting is that the phosphate counterions layer under the surface must have been surprisingly dense. Both the intensity of the bands and the width of the splitting thus acted as an indicator of peptide adsorption below DPPC heads. This indicator, although indirect, had a considerable advantage of being insensitive to the peptide orientation.

The first injection of peptide ($c = 0.1$ μM) was enough to nearly saturate the spectrum, with $I'_{1,or}$ and I'_2 reaching more than 50% of their maximal values, and to induce a drastic 6-fold decrease in the lipid $\nu(C=O)$, ν_a and $\nu_s(CD_2)$ bands (Fig. 10c). Note that under a neutral lipid monolayer, the peptide was barely visible at this concentration! Making a layer with 25% DPPS mixed to DPPC, or even 100% DPPS, did not significantly affect these measurements.

To visualise an intermediate spectrum was possible only within a few minutes after injection: the phosphate band was already saturated, but not the peptide, reflecting its slower adsorption kinetics (see Fig. 10a,b). Note that, at low peptide concentration, the percentage of antiparallel β-sheets amounted to 89%

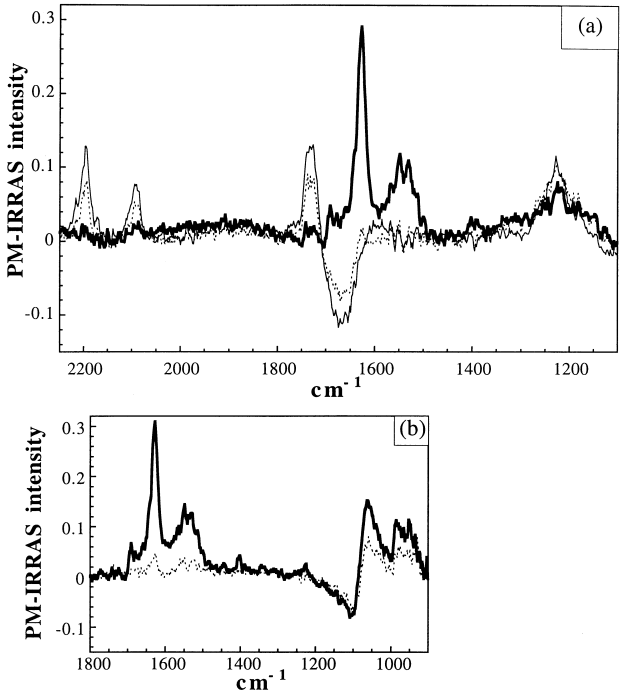

Fig. 10. Spectroscopic data of mixed peptide and 90% DPPC+10% DPPS lipids. (a) Spectra of a lipid film at 13 mN/m with peptide injected at bulk concentration $c = 0.1$ μM. Thin solid line: equilibrium spectrum of lipids only (shown for comparison). Dots: transient spectrum recorded between 6 and 16 min after injection; thick line: spectrum recorded between 19 and 29 min after injection. (b) Same spectra after subtraction of the area normalised lipid spectrum. The phosphate band due to PBS was already saturated before 16 min (dots) and presents a TO–LO splitting; the peptide bands were saturated after 19 min (thick line, identical to an equilibrium spectrum recorded after 30 min). (c) Analysis of the spectra vs. peptide concentration: same legend as Fig. 8c.

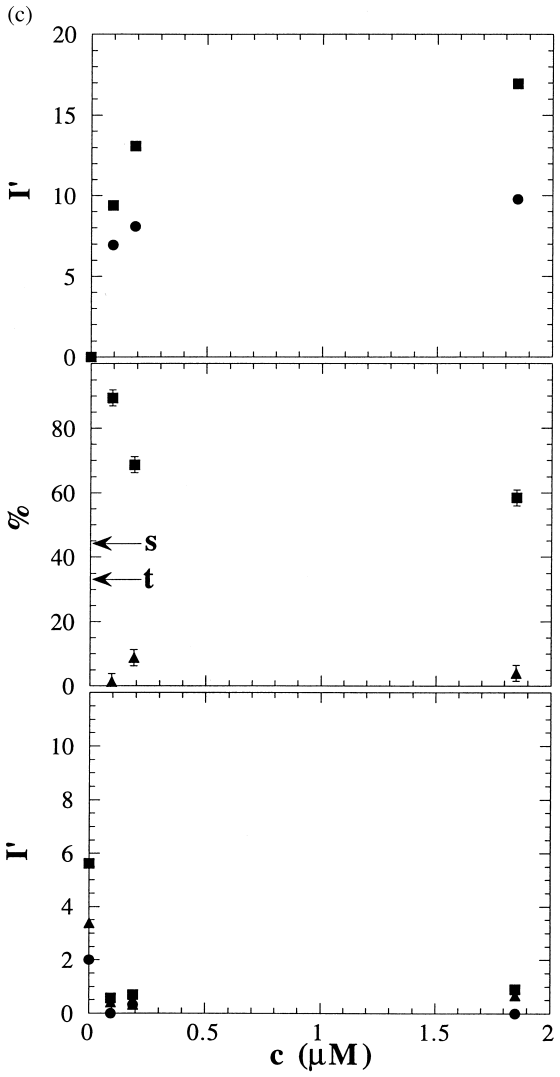

Fig. 10 (*continued*).

while β-turns fell down to an insignificant 1% and others contributed to 9% (Fig. 10c). Both I'_{1628} and especially I'_{1690} decreased with respect to the peptide alone, indicating a large xX tilt and a side inclination yY. At high peptide concentration, antiparallel β-sheets fell to 58% and the β-turns contribution remained barely significant at 4%. I'_{1628} remained low, but not I'_{1690}, indicating that the tilt (xX) had probably vanished.

Finally, while compressing the lipid+peptide film up to 27 mN/m, the monolayer did not resist compression, the area slowly decreasing with time: not only was the peptide ejected into the water, but also did it apparently partially solubilise the lipids.

4. Discussion

4.1. Surface activity of the peptide

4.1.1. Pure peptide

Despite its adsorption time-scale of less than 15 s (Fig. 2), the pure peptide monolayer has a very long time-scale of lateral equilibration, typically 10–20 min. During compressions and decompressions it is largely out of equilibrium, resulting in a large hysteresis in pressure (Fig. 4), but not in spectra. The adsorbed peptide is visible in the surface pressure at a concentration of 0.4 μM and even lower in IR spectra. The absolute amount of peptide at the sur-

Table 4
Surface activity of the natural 16 residue peptide 'penetratin'

Peptide	$c_{2\,(}$μM)	c_d (μM)	K_p	Π_{max} (mN/m)	Π_c (mN/m)
Penetratin	0.2	1.5	0.25	26	≤27
LK_{15}	0.035	0.4	1.4	32	>35

c_2 and c_d are the peptide bulk concentrations to reach $\Pi = 2$ mN/m, or a dense monolayer, at which the partition coefficient K_p between surface and bulk was determined. Π_{max} was the highest surface pressure reached by successive injections, Π_c the critical lipid pressure for peptide insertion. All criteria show that its surface activity is smaller than the synthetic 15 residue amphiphilic peptide LK_{15} studied in [9], indicated for comparison. Note that c_d was determined by the saturation of the ellipsometric angle for penetratin, and of surface pressure for LK_{15}.

face can be determined from the ellipsometric angle Δ only under a simplistic linear assumption; for instance a proportionality constant of order 0.2 mg/m^2 per degree [19] would indicate a partition coefficient $K_p = 25\%$ between peptide at air–water interface and in the bulk subphase.

Quantitatively, the surface activity of the peptide is systematically lower than a synthetic amphiphilic peptide of comparable length, the LK_{15} (see Table 4) [9].

4.1.2. Peptide with lipids

From the interaction of the peptide with different lipids and at different surface pressure we can extract the following conclusions.

At high DPPC density $\Pi_{lip} = 27$ mN/m, the layer thickness measured by ellipsometry and its variation with surface tension seem entirely controlled by the lipid, as if the peptide was expelled from the water surface.

At $\Pi_{lip} = 13$ mN/m, the peptide interacts both with neutral and negatively charged lipid films. Modifications in the infrared spectra are detected at low concentrations: 0.1 μM for pure DPPC (Fig. 8a), even lower with 10% DPPS (for $c = 0.1$ μM the spectrum is nearly completely saturated) (Fig. 10a). This reveals a high affinity of the peptide for these lipids. If we now analyse only the monolayer at the surface, we can see that the film area A varies linearly with the bulk peptide concentration c (Fig. 7). Under the assumption that all the increase in area can be attributed to an increase in the number of peptide molecules (and not to an increase in lipid molecular area), and that the molecular area is of about 260 Å^2 (corresponding to a 16 residue β-sheet peptide molecule [9]), it is possible to calculate the partition coefficient between bulk and surface which are very low: only 0.7% of the injected peptide inserts into the pure DPPC monolayer and 1.6% with 10% DPPS. The total amount of peptide detected in spectroscopy, i.e. both between and below the lipids, is obviously much higher. Indeed, the peptide seems to be firmly adsorbed below the heads of the DPPS in the monolayer, and might itself be assembled into a stable parallel layer in the water. This is not unlikely, given the electrostatic interaction between the seven positive charges of a peptide molecule and the negative charge of a DPPS head: the peptide would adsorb strongly but would not insert into the layer. Such a picture is supported by the formation of a densely packed phosphate counter-ion monolayer under the monolayer. More detailed information on the peptide insertion would require experiments at peptide concentration small enough to prevent the saturation of amide bands.

4.2. Structure of the peptide

The structure of the pure peptide is dominated by antiparallel β-sheets which could be favoured by the local alternance of hydrophilic and hydrophobic residues. Since the 1628 cm^{-1} frequency remained constant even at high pressures, we can exclude the existence of a transition towards parallel sheets. The β-sheet/β-turn ratio around 4 suggests that most molecules assume the shape of an amphiphilic hairpin (Fig. 9), i.e. the antiparallel β-sheets are intra-molecular. The twist could then be centred on the middle of the molecule, namely Gln-Asn, or even extend to the Arg-Arg pair. This structure can be mildly stabilised by the interaction of hydrophobic residues and keep a residual plasticity. It probably presents a static disorder (the order is broken in parts of the molecule all of the time), or a dynamic one (the disorder

is part of the time, over the whole molecule), resulting in intra- or inter-molecular disorder. There are 13% other structures (and up to 25% at high pressure): random coils and α-helices evidenced by a weak component around 1644–1650 cm^{-1}. Since the 1300 cm^{-1} band is intrinsically weak, and could vanish simply due to orientation effects, its absence does not indicate that α-helices are absent.

Neutral lipids decrease the importance of the β structure, which might mean that the 'hairpin' becomes less stable, resulting in an increased disorder. Charged lipids maintain a strikingly high proportion (Fig. 10c) of antiparallel β-sheets. Conversely, the 1679 cm^{-1} β-turn band disappears. This cannot be explained by orientation corrections alone. We could thus conclude that charged lipids induce disorder (like neutral lipids), mostly around the twist of the hairpin. Since no parallel β-sheets are detected, there is no sign of any inter-molecular association, i.e. oligomerisation, making for the loss of intra-molecular organisation. Despite the high proportion of β-sheet bands, it seems that the peptide, too short to maintain a stable secondary structure, increases its flexibility according to its environment.

4.3. Orientation of peptide and lipids

The pure peptide molecule lays flat on the water surface. This probably optimises the unfavourable hydrophilic–hydrophobic interactions, which such a short peptide cannot reduce by self-association only. Like for the synthetic LK_{15} observed in [9], this result is roughly pressure-independent.

When inserting into a lipid monolayer at 13 mN/m, the peptide lies along its side, and even tilts with charged lipids at low pressure. With DPPC, it strongly tilts the lipid chains, moderately affects the esters and does not affect the heads (Fig. 8c): thus the peptide probably inserts between chains. Conversely, its effect on the charged monolayers (Fig. 10c) is much more drastic and results in a total disorder of the whole lipid structure. This is exactly what has been observed on the same peptide in a planar bilayer by neutron reflectivity [12]: the peptide induced a low chain disorder in a neutral DPPC bilayer, and strongly disordered the whole structure of a 10% DPPS charged bilayer. This behaviour is rather atypical, since it is not collective (like the oligomerisation of pore-forming peptides, see e.g. [8,20]) and it does not lead to the formation of separated peptide and unperturbed lipid domains [9].

5. Conclusion

Due to their small size and the variability of their structures, peptides are difficult to study directly in situ while interacting with lipids. In the present paper, we have shown how surface infrared spectra, ellipsometric angle and surface pressure yield complementary information on the adsorption of penetratin under a lipid monolayer: quantitative measurements of absorption amount and kinetics, determination of peptide configuration, peptide orientation and lipid orientation. We obtained the following conclusions:

- Penetratin has a high surface activity.
- Its adsorption under lipids is mostly affected by electrostatic attraction towards lipid heads. With negative charges in the heads, its action on lipids is qualitatively modified: the peptide inserted less between lipid tails, and instead induced a significant disorder in orientation of lipid heads and tails. This is consistent with observations by neutron reflectivity on a lipid bilayer [12]. One might speculate that the translocation properties of the penetratin are linked with the disorder it induces in (charged) lipid layers.
- The peptide secondary structure is dominated by β-structures, especially in the presence of charged lipids. This contrasts with its helical structure within the native Antennapedia homeodomain [1].
- With its hairpin-like shape, the peptide keeps some plasticity, and can also tilt away from the layer plane to insert between lipids. These features may also play a role in its translocation [21].
- No collective behaviour such as oligomerisation nor pressure-dependent reorganisation has been detected.

Acknowledgements

F.G. thanks A. Prochiantz and D. Derossi for an introduction to the properties of penetratin, and nu-

merous discussions which are at the origin of this work. We would like to thank J.-F. Hernandez, Y. Pétillot and E. Le Calvez for their help and discussions.

References

[1] Y.Q. Qian, M. Billeter, G. Otting, M. Müller, W.J. Gehring, K. Wührich, Cell 59 (1989) 573–580.
[2] D. Derossi, A. Joliot, G. Chassaing, A. Prochiantz, J. Biol. Chem. 269 (1994) 10444–10450.
[3] J. Brugidou, Ch. Legrand, J. Méry, A. Rabié, Biochem. Biophys. Res. Commun. 214 (1995) 685–693.
[4] D. Derossi, S. Calvet, A. Trembleau, A. Brunissen, G. Chassaing, A. Prochiantz, J. Biol. Chem. 271 (1996) 18188–18193.
[5] A. Prochiantz, Curr. Opin. Neurobiol. 6 (1996) 629–634.
[6] R. Fåhraeus, J. Paramio, K. Ball, S. Lain, D. Lane, Curr. Biol. 6 (1996) 84–91.
[7] E.T. Kaiser, F.J. Kézdy, Annu. Rev. Biophys. Biophys. Chem. 10 (1987) 561–581.
[8] I. Cornut, E. Thiaudière, J. Dufourcq, The amphipatic helix in cytotoxic peptides, in: R.M. Epand (Ed.), The Amphipatic Helix, CRC Press, Boca Raton, FL, 1993, pp. 173–219.
[9] S. Castano, B. Desbat, M. Laguerre, J. Dufourcq, Biochim. Biophys. Acta 1416 (1999) 176–194.
[10] D. Blaudez, T. Buffeteau, J.C. Cornut, B. Desbat, N. Escafre, M. Pezolet, J.M. Turlet, Appl. Spectrosc. 47 (1993) 869–874.
[11] D. Blaudez, J.M. Turlet, J. Dufourcq, D. Bard, T. Buffeteau, B. Desbat, J. Chem. Soc. Faraday Trans. 94 (1996) 525–530.
[12] G. Fragneto, F. Graner, T. Charitat, P. Dubos, E. Bellet-Amalric, Langmuir 16 (2000) 4581–4588.
[13] E.T. Buffeteau, E. LeCalvez, S. Castano, B. Desbat, D. Blaudez, J. Dufourcq, J. Phys. Chem. B 104 (2000) 4537–4544.
[14] B. Berge, A. Renault, Europhys. Lett. 21 (1993) 773–777.
[15] R.M.A. Azzam, N.M. Bashara, in: Ellipsomety and Polarized Light, North Holland personal library, Amsterdam, 1977.
[16] S. Castano, B. Desbat, J. Dufourcq, Biochim. Biophys. Acta 1463 (2000) 65–80.
[17] A. St-Jalmes, F. Graner, F. Gallet, B. Houchmandzadeh, Europhys. Lett. 28 (1994) 565–571.
[18] M. Balkanski, in: F. Abelès (Ed.), The Optical Properties of Solids, North-Holland, Amsterdam, 1972, Ch. 8.
[19] J.A. de Feijter, J. Benjamins, F.A. Veer, Biopolymers 17 (1978) 1759–1772.
[20] Y. Wu, K. He, S. Ludtke, H. Huang, Biophys. J. 68 (1995) 2361–2369.
[21] P.D. Kwong, R. Wyatt, J. Robinson, R.W. Sweet, J. Sodroski, W.A. Hendrickson, Nature 398 (1998) 648–659.